Numerical Analysis of Cavitating Flow over A2d Symmetrical Hydrofoil

[1,] Greeshma P Rao , [2,] Likith K, [3,] Mohammed Naveed Akram, [4]Adarsh Hiriyannaiah

[1,2,3,4] Department of Mechanical Engineering R V College of Engineering, Bangalore

Abstract

This report presents the numerical investigations of cavitating flow over a 2D symmetrical hydrofoil. Turbulent cavitating flow over a hydrofoil is simulated using a transport equation based model with consideration of the influence of non condensable gases. The results presented in this report focuses on Cavitation inception, shape and behaviour of sheet cavity, lift and drag forces with cavitation and the pressure distribution around the foil. Steady and unsteady simulations are carried out at different cavitation numbers ranging from near inception conditions to developed conditions and almost super cavitating conditions. Standard k-ε model without any modifications are used for simplicity. Effect of dissolved gas content is also considered.

Index Terms— Cavitation, Hydrofoil, Standard k-ε model.

I. INTRODUCTION

Cavitation is defined as the process of formation of the vapour phase of a liquid when it is subjected to reduced pressures at constant ambient temperature. Thus, it is the process of the boiling in a liquid as a result of pressure reduction rather than heat addition. However, the basic physical and1, 2 :UndergraduateStudents(UG)4Assistant professor (RVCE)thermodynamic processes are the same in both cases. A liquid is said to cavitate hen vapour bubbles form and grow as a consequence of pressure reduction.When the phase transition results from hydrodynamic pressure changes, the two-phase flow composed of a liquid and its vapour is called a 'cavitating flow'. Cavitation flow may be seen (and heard) as water flows through a glass venturi tube (fig 1), an experiment first exhibited by Osborne Reynolds in 1894. According to Bernoulli's equation, when the velocity increases, the pressure decreases. At sufficiently high flow rates the liquid in the throat begins to boil, because the velocity is highest and the pressure is lowest at this section. The small
bubbles formed there are filled with cold steam and other gases diffused from the liquid. [1]

Hydrofoil

Hydrofoils are foils operating in liquid medium. They need not be as large as an aerofoil due to higher density of Liquid than air. They help in increasing the performance of machines

Adverse Effects of Cavitation

The main effects of cavitation are adverse effects: noise, erosion, vibrations and disruption of the flow, which results in loss of lift and increase of drag. Cavitation is known for its violent behaviour. That is caused by the fact that vaporization of water and condensation of vapour are very fast processes, much faster than the dynamics of a vapour cavity. As a result the growth and collapse of a cavity is not slowed down by these processes. Because cavitation is part of the flow, it can move rapidly from regions of low pressure into regions of a higher pressure. This leads to a very rapid collapse. The collapse is so rapid that the local speed of sound in the fluid is exceeded and shock waves occur. The consequence is that cavitation generates noise over a wide range of frequencies, especially higher frequencies. Also the local pressure rises very strongly at collapse, leading to damage of adjacent surface. This effect is called erosion. When larger amounts of vapour are involved the implosion of cavitation can cause pressure variations in the fluid, which lead to vibrations of the cavitating structure. Cavitation can also alter the flow. This is the case on propellers when the cavitation becomes extensive. In that case the flow over the blades and the lift of the blades is altered by cavitation and the thrust of the propeller is strongly reduced. This is called 'thrust breakdown'. In valves cavitation can also block or choke the flow. The volume of vapour in cavitation is much larger than the volume of water that has evaporated. In cases of extensive cavitation this leads to large volume increases and decreases when cavitation grows and collapses. The volume variations cause pressure fluctuations in the surrounding fluid, resulting in structural vibrations. The properties of cavitation and its implosion can also be used, as mentioned below.

2. Cavitation number

Generally tests are carried out in a cavitation tunnel. In this case the easiest parameters to measure are:low velocity, pressure upstream of hydrofoilIt is customary to define σ by the following expression

$$\sigma = \frac{P_{up} - P_v}{\frac{1}{2}\rho V^2}$$

$$C_p = (p_v - p_b) / (0.5\rho v^2)$$

Figure 2.1

The following figures (2.1, 2.2(a), 2.2(b), 2.2(c)) [3] show the relation between pressure coefficient c_p and cavitation number σ for non cavitating, possible cavitation and developed cavitating conditions

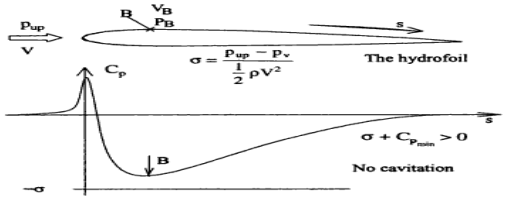

Figure 2.2(a)

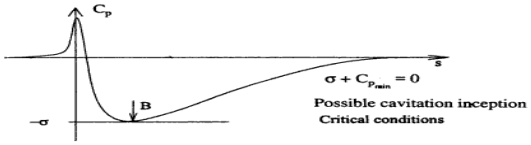

Figure 2.2(b)

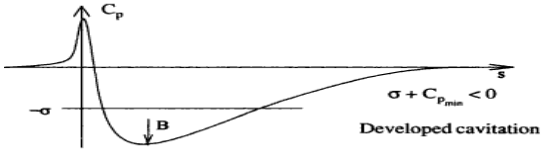

Figure 2.2(c)

3. Cavitation Simulation

Cavitation is a two phase flow occurring in a liquid when the local static pressure falls below the vapour pressure corresponding to the liquid temperature. It affects the performance of hydraulic machines. Need for understanding cavitation in turbo machines is thus apparent. Because of experimental difficulties, simulation could be a useful tool to understand cavitation in such applications Simulating the occurrence of cavitation in a hydraulic machine is a challenging task because of the complex flow phenomenon as well as the complicated geometry of hydro turbo machines; usually new cavitation models are tested against experimental data obtained from much simpler geometry. One such flow simulation widely used to validate numerical approach is the flow over a hydrofoil. Hydrofoils form the basics of impeller blades of axial flow machines. Thus information of cavitation on a hydrofoil yields useful information about axial machine performance under cavitation.

Simulation of cavitation requires a coupling between Navier-stokes equation, physical model for cavitation and closure model for turbulence. Moreover such flows are systematically unsteady at some scale thus an effective cavitation model is needed to correctly take into account the different flow phenomenon Kubota et al[6] proposed a new cavity model (bubble two-phase flow) that can express well the interactions between vortices and bubbles. Rebound et al [7] have investigated the ability of two-equation turbulence models to reproduce the cavity unsteadiness in the case of a venturi nozzle. They have stated that the use of the k- ε turbulence model leads to steady-state cavity because of the high turbulent viscosity level induced by the turbulence model. Singhal et al [8] developed the full cavitation model in which the phase change expressions are derived from a reduced form of a Rayleigh-Plesset equation. The numerical model has been applied to the 2D configuration (fig 8.4).

The flows corresponding to different cavitation numbers have been investigated, to obtain successively non cavitating flow, steady and unsteady sheet cavitation (cloud cavitation), finally supercavitation flow.

4. Mathematical Models Multi-Phase Model

The multi-phase mixture model in FLUENT14.0 assumes that the working medium is a single fluid with a homogeneous mixture of two phases (liquid and vapour). Therefore, only one set of RANS equations is solved for the mixture fluid. Denoting the density of the mixture fluid by ρ_m, the continuity equation for the mixture flow becomes:

$$\frac{\partial}{\partial t}(\rho_m)+\nabla\cdot(\rho_m\vec{v}_m)=0$$

The momentum equation for the mixture reads:

$$\frac{\partial}{\partial t}(\rho_m\vec{v}_m)+\nabla\cdot(\rho_m\vec{v}_m\vec{v}_m)$$
$$=-\nabla p+\nabla\cdot\left[\mu_m\left(\nabla\vec{v}_m+\nabla\vec{v}_m^T\right)\right]+\rho_m\vec{g}+\vec{F}$$

The density constitution of each phase in a mixture-flow cell is described by means of a scalar volume fraction. The relation between different volume fractions is linked by:

$$\rho_m=\alpha_v\rho_v+(1-\alpha_v)\rho_l$$

Where α_v and α_l are the volume fraction of vapour and liquid respectively. To close the equations an additional transport equation is solved for α_v. To account for the mass transfer between phases a cavitation model is needed, as discussed below.

Cavitation Model

Singhal et al cavitation model [8]This cavitation model is based on the "full cavitation model", developed by Singhal et al. It accounts for all first-order effects (i.e., phase change, bubble dynamics, turbulent pressure fluctuations, and non- condensable gases). It has the capability to account for multiphase (N-phase) flows or flows with multiphase species transport, the effects of slip velocities between the liquid and gaseous phases, and the thermal effects and compressibility of both liquid and gas phases. The cavitation model can be used with the mixture multiphase model, with or without slip velocities. However, it is always preferable to solve for cavitation

using the mixture model without slip velocity; slip velocities can be turned on if the problem suggests that there is significant slip between phases.

To derive an expression of the net phase change rate, Singhal et al uses the following two-phase continuity equations

Liquid phase:

$$\frac{\partial}{\partial t}[(1-\alpha)\rho_\ell] + \nabla.[(1-\alpha)\rho_\ell \vec{V}] = -R$$

Vapour phase:

$$\frac{\partial}{\partial t}(\alpha\rho_v) + \nabla.(\alpha\rho_v \vec{V}) = R$$

Mixture:

$$\frac{\partial}{\partial t}(\rho) + \nabla.(\rho\vec{V}) = 0$$

The expression for the net phase change rate (R) is finally obtained as

$$R = (n4\pi)^{\frac{1}{3}}(3\alpha)^{\frac{2}{3}}\frac{\rho_v\rho_\ell}{\rho}[\frac{2}{3}(\frac{P_B - P}{\rho_\ell})]^{\frac{1}{2}}$$

Singhal et al. proposed a model where the vapour mass fraction is the dependent variable in the transport equation. This model accommodates also a single phase formulation where the governing equations are given by:

$$\frac{\partial}{\partial t}(f_v\rho) + \nabla.(f_v\rho\vec{V}_v) = \nabla.(\Gamma\nabla f_v) + R_e - R_c$$

Turbulence modelling [4]

In this simulation standard k ε model without any modifications is tested and it q has been found that this yields to inaccurate predictions especially in near wall conditions. For this model the transport equation for k is derived from the exact equation, but the transport for ε was obtained using physical reasoning and is therefore similar to the mathematically derived transport equation of k , but is not exact. The turbulent kinetic energy k and its rate of dissipation ε, for this model are obtained by the following equations.

$$\rho u_j \frac{\partial k}{\partial x_j} = \rho\tau_{ij}\frac{\partial u_i}{\partial x_j} + \frac{\partial}{\partial x_j}\left[\left(\mu + \frac{\mu_T}{\sigma_k}\right)\frac{\partial k}{\partial x_j}\right] - \left[\rho\varepsilon + 2\mu\left(\frac{\partial k^{1/2}}{\partial x_j}\right)^2\right]$$

$$\rho u_j \frac{\partial k}{\partial x_j} = \rho\tau_{ij}\frac{\partial u_i}{\partial x_j} + \frac{\partial}{\partial x_j}\left[\left(\mu + \frac{\mu_T}{\sigma_k}\right)\frac{\partial k}{\partial x_j}\right] - \left[\rho\varepsilon + 2\mu\left(\frac{\partial k^{1/2}}{\partial x_j}\right)^2\right]$$

$$\rho u_j \frac{\partial \varepsilon}{\partial x_j} = C_1\frac{\varepsilon}{k}\tau_{ij}\frac{\partial u_i}{\partial x_j} + \frac{\partial}{\partial x_j}\left[\left(\mu + \frac{\mu_T}{\sigma_\varepsilon}\right)\frac{\partial \varepsilon}{\partial x_j}\right] - C_2\frac{\rho\varepsilon^2}{k} + \frac{2\mu\mu_T}{\rho}\left(\frac{\partial^2 u}{\partial x_2^2}\right)^2$$

5. Procedure in ansys fluent

Geometry and Meshing

The shape of the hydrofoil is given by

$Y/c=a_0(x/c)^{1/2}+a_1(x/c)+a_2(x/c)^2+a_3(x/c)^3+a_4(x/c)^4$

Where a_0=0.11858, a_1=-0.02972, a_2=0.00593, a_3=-0.07272,a_4=-0.02207

The geometry is created by using the equation above. And the surface is created from the curve obtained by the coordinates satisfying the above equations.

Final surface is shown in fig (5.1.1)

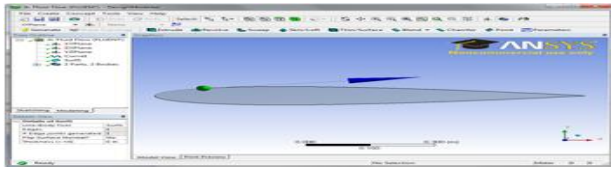

Fig 5.1.1

The foil is 1m long in chord and maximum width 0.12m.The dimensions of the arc of the c mesh is 12.5 m and length of the rectangular part is 12.5m with the trailing edge of the hydrofoil situated at the centre of the arc.

Once the c mesh outline is created a second surface (target body) is generated from this a hydrofoil surface is subtracted (tool body) shown in figure (5.1.2)

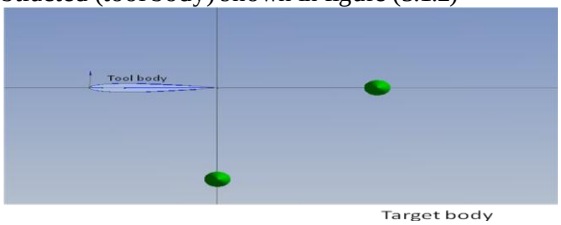

Figure 5.1.2

Then the obtained surface is spilt into 4 quadrants to facilitate easy meshing.

The mesh is generated using mapped face meshing and suitable edge sizing

Thus obtained mesh is as shown below

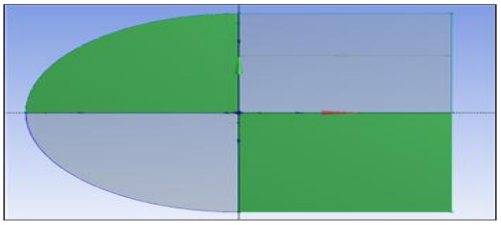

Figure 5.1.3

Computational domain

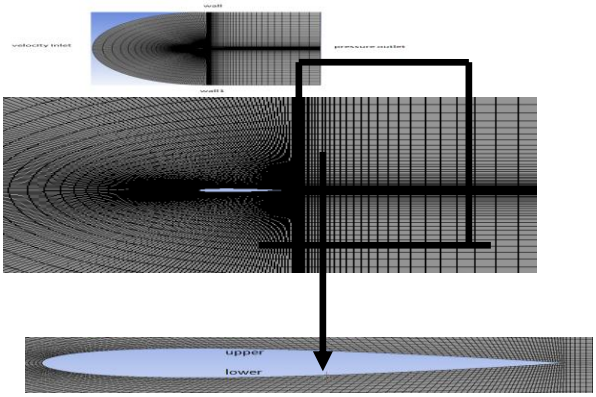

Fig 5.2

Solution set up- Grid and Boundary conditions

The foil has a 7° angle of attack (AoA) that is the flow is inclined at 7° and is operated at and is operated at various cavitation numbers. Table 1 gives the flow and boundary conditions. The physical properties for the liquid and the vapor in Table 1 correspond to a water temperature at 27°C

Table 1 – Boundary Conditions

Boundary conditions	values	
Upstream: constant velocity inlet, [m/s]	6	
turbulent intensity [%]	1	
turbulent viscosity ratio [-]	8	
Downstream: pressure outlet, [kPa] (gauge)	0	
Foil surface: No-slip	-	
Tunnel wall: Slip	-	
Physical properties of water	**Vapor**	**liquid**
Vaporization pressure, [kPa]	2.3678	
Dynamic viscosity, [kg/ms]	0.0000134	0.001003
Density, [kg/m3]	0.5542	998.2

Table 2 Information on grids for hydrofoil

Nodes	Elements	Level
15300	15000	Coarse

Table 3

Cavitation number	Pressure upstream(gauge)kpa
5	9119.2
4	27086.8
3	45054.4
2.5	54038.2
2	63022.6
0.9	82786.36
0.55	89075.02

6. Results and discussions

For 7° angle of attack after the numerical simulations for a wide range of operating pressures the following five main flow configurations have been observed in the system

- Non cavitating flow(σ>4)
- Near cavitation inception(σ=3)
- Sheet cavitation(α from 2 to 3)
- Sheet cavitation(σ=0.9)
- Near super cavitation(σ=0.55)

The c_{pmin} value is -2.375 for σ=4(figure 6.1)
Since the c_p curve does not cross the –σ line the cavitation does not happen. Hence σ=4 is for non cavitating conditions.
The cavitation begins at about σ=3.5 but is prominently noticed at σ=3 and this leads to developed cavitation at σ=2.5 followed by σ=2.at lower cavitation numbers i.e...σ = 0.55, 0.9 etc the cavitation gets unsteady or cloud cavitation. For σ=3 c_p curve does crosses the –σ line the cavitation happens. Hence σ=3cavitation begins. (figure8.2) Cp v/s position for σ=2, that is developed cavitation (figure 6.3)
However cavitation itself is an unsteady phenomenon (transient flow) and hence we can speak only of degree of unsteadiness in the flow.

Development of cavity

Sheet cavitation occurs when there is a strong low pressure peak at the leading edge of the foil and sheet cavitation therefore has its leading edge close to the leading edge of the foil. The closure of the cavity is shown in Fig6.7.At the beginning or leading edge of the cavity, constant pressure means that the streamlines separate tangentially from the surface of the foil at point A (assuming that the foil is a smooth surface). Tangential separation, however, means that there is a region just downstreamof the separation location where the cavity is very thin, so thin that the surface tension becomes recognizable and results in a curved surface, making the leading edge of the cavity at point B instead of A.
Also point B experiences the lowest pressure marking the beginning of the cavity. (Indicated by red regions) The space around point A encounters flow separation leading to reduced volume of vapour at that point, indicated by yellow region (also near the trailing edge), The phase contours for σ=3 is plotted for different times. The fig (6.4, 6.5, 6.6), shows a few plots for 300,500,700ms are shown. The vapour reaches a maximum volume fraction of 1.91x10^-2 in 500 ms.

Phase contours

For σ=2 the phase contours are plotted fig (6.8, 6.9, 6.10,6.11)And reaches a maximum vapour volumefractionof2.03x10^-2 at 500ms which is greater than that ofσ=3.Also the length of the cavity is increased.
For σ=0.9 the phase contours are plotted –fig(6.12, 6.13, 6.14, 6.15) And reaches a maximum vapour volume fraction of 2.18x10^-2 at 450 ms. The vapour content is greater and reaches a maximum at a faster rate indicating that the cavitation gets more unsteady. Also the length of the cavity is increased.For the phase contour for σ=0.55 the maximum vapour volume fraction is 2.21x10^-2
which is reached at 500ms which is greater than the previous vapour factions. The fig (6.19) illustrates the vapour shedding at 168.2ms The vapour shedding takes place even before the full development of the cavity which indicates that the shedding of the cavity takes place by parts and not as a whole which is an example for unsteady cloud cavitation.

Effect of cavitation on lift and drag

The drag coefficient c_d is defined as:

$$c_\mathrm{d} = \frac{2F_\mathrm{d}}{\rho v^2 A},$$

Where:

F_d Is the drag force, which is by definition the force component in the direction of the flow velocity.
ρ is the mass density of the fluid,
v is the speed of the object relative to the fluid and
A is the reference area or projected area

The lift coefficient C_L is equal to:

$$C_L = \frac{L}{\frac{1}{2}\rho v^2 A} = \frac{2L}{\rho v^2 A} = \frac{L}{qA}$$

Where

L is the lift_force, ρ is fluid density, $\vec{v}$ is true airspeed, q is dynamic pressure and A is plan form area. Or projected area

The plots (Figure 6.20 (a) & (b)) show the lift and drag coefficient during the incipient flow for various cavitation numbers.

We observe that the lift coefficient decreases and drag co efficient increases with decrease in cavitation number .indicating increase in drag force and decrease in lift force with cavitation.

The Graphs figs (6.21 (a), (b), (c)) show the variation of absolute pressure with respect to position on the hydro foil, for cavitation numbers 0.9 We observe that the absolute pressure distribution over lower surface remains same however the pressure distribution over the upper surface changes. It has observed that the area between the two curves decreases as the cavitation number decreases indicating decrease in lift force as

Effect of dissolved gas content For Cavitation number 0.9 and gas content 5, 10, 15 and 20ppm

Graphs 6.23(b),6.23(c),6.23(d) represents the variation of c_p with different dissolved gas contents. we observe that with the incresing gas content(from 10ppm to 20ppm) the value of cpmin falls, indicating that the conditions get more favorable to cavitation. On the contrary the value of cpmin for 5ppm(6.23 (a)) is lower than that of 10ppm. This is probaly because very low gas content lead to lesser nuclei in water which may lead to bubble cavitation which is a stronger form of cavitation than sheet cavittion , justifying the fall in cpmin.Hence high nuclei density is favorable for sheet cavitation while low nuclei density l leads to bubble cavitation

Conclusions

Cavitation is a phenomenon that has adverse affects on the performance and life of the hydraullic machines, making it an inevitable subject of study.Analysisng cavitation can provide us information,about the sites vulnerable to cavitation damage and therefore help us to take suitable measures for its prevention.

The phenomenon is known to have a devastating effect on the blades of the impellers used in various fluid machinery. Therefore the investigation of the phenomenon over different blade profiles is a cynosure of cavitation studies.

Hydrofoil is one of the simplest and most widely used profiles in impellers for axial flow machines. In the analysis of a 2 D symetrical hydrofoil it is observed that by decreasing cavitation number, different cavitation regimes are formed.The near cavitation inception is obtained at 3 to 3.5 after which cavitation is developed and subsequently becomes unsteady. Cloud cavitation occurs at a cavitation number of 0.55. Further increase in cavitation number leads to supercavitation conditions. It is also seen that the regions close to leading edge are sites susceptible to this phenomenon. It is observed from simulations that gas content also has a major effect on the cavitation formation. Lift decreases and drag increases with the increase in cavitation.(which can thwart the performance of the machinery).

Further the standard turbulence model k-ε used, without any modification is not very accurate in predicting the phase contours, vapour shedding and near wall conditions.

In future the investigation can be extended to study the phenomenon for various angles of attack with modifications of models used to improve the accuracy and reliability of the results.

Bibliography

1. Cavitation "section 12, handbook of fluid mechanics, McGraw-hill BookCo., Inc., 1961(section 12-I:"mechanics of cavitation," by Phillip Eisenberg; section I2-II:"supercavitating flows", by Marshall P Tulin)
2. Bertin, John and Michael Smith; Aerodynamics for Engineers, Third Edition. Prentice Hall: New Jersey, 1998.
3. Cavitation Bubble Trackers" BY Yves Lecoffre (2009)
4. Pope, S.B., 'Turbulent Flows', (2000)

References

1. Introduction to Cavitation and Supercavitation Paper presented at the RTO AVT Lecture Series on "Supercavitating Flows", held at the von Kármán Institute (VKI) in Brussels, Belgium, 12-16 February 2001, and published in RTO EN-010.
2. Kubota a Kato, and Yamaguchi, H 1992, A new modelling of cavitating flows; a numerical study of unsteady cavitation on a hydrofoil section, J Fluid mech.240, pp 59-96
3. Rebound J. L., Stutz B., and Coutier- Delgosha, o., 1998, two phase flow structure of cavitation: experiment and modelling of unsteady effects. Pre, oct 3rd int.
4. Singhal A K Athavale M .M., Li ,H .Yi., and Jiang Y 2002, mathematical basis and validation of full cavitation model J. Fluid Engg, 124, pp 617-624
5. "Introduction to CFD Basics", Rajesh Bhaskaran, Lance Collins (2010)
6. ranc J.P. and Michel J.M. (2004) "Fundamentals of cavitation" *Kluwer*.
7. Kato H. (1984) "Thermodynamic effect on incipient and developed sheet cavitation" *Proc. Int. Symp. On Cavitation inception, FED-Vol.16,* New-Orleans (USA), Dec. 9-14, 1984, 127-136.
8. A. Ducoin, J. A. Astolfi, F. Deniset, and J.-F. Sigrist, "Computational and experimental investigation of flow over a transient pitching hydrofoil," *European Journal of Mechanics B*, vol. 28, no. 6, pp. 728–743, 2009

9. M. Morgut, E. Nobile, and I. Biluš, "Comparison of mass transfer models for the numerical prediction of sheet cavitation around a hydrofoil," *International Journal of Multiphase Flow*, vol. 37, no. 6, pp. 620–626, 2011.
10. G.Kuiper, Cavitation in Ship Propulsion, January 15, 2010
11. Stepanoff A.J. (1964) "Cavitation properties of liquids" *J. of Eng. for Power*, April 1964, 195-200.
12. Numerical and experimental study on unsteady shedding of partial cavitation (2009) BIN JIn XIANWU LUO† and YULIN WU
13. 5. J. Choi, C. T. Hsiao, G. Chahine and S. Ceccio, *J. Fluid Mech*. 624 (2009) 255.
14. 8. B. Ji, F. W. Hong and X. X. Peng, *Journal of Hydrodynamics, Ser. A* 23(04) (2009) 412.
15. De Lange D.F. & De Bruin G.J. (1998) "Sheet cavitation and cloud cavitation, re-entrant jet and threedimensionality" *Appl. Sci. Res.* 58, 91-114.
16. MODELING OF CAVITATION FLOW ON NACA 0015 HYDROFOIL(2009) Jaroslav ˇStigler*, Jan Svozil*

Appendix A

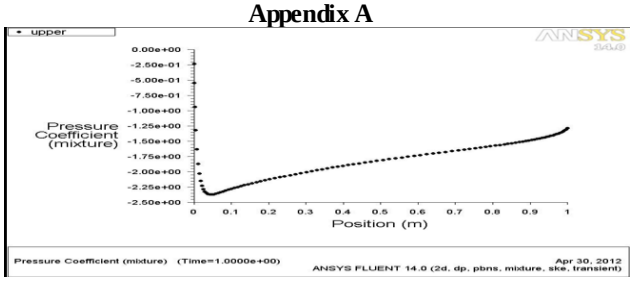

Figure 1

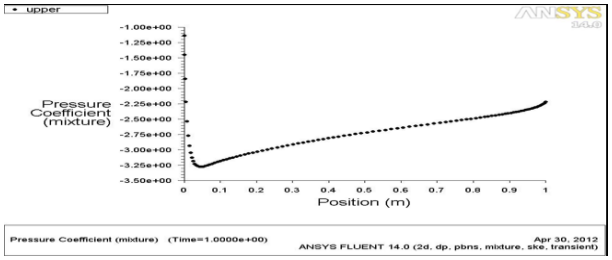

Figure 2

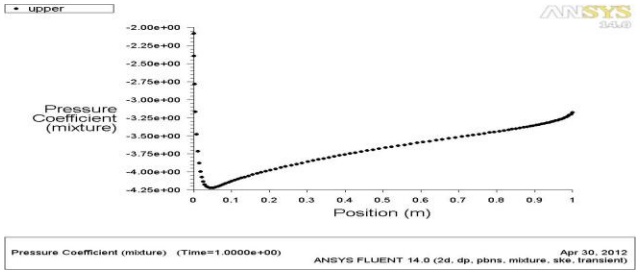

Figure 3

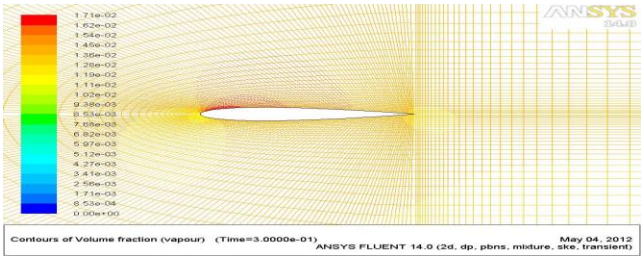

Figure 8.4

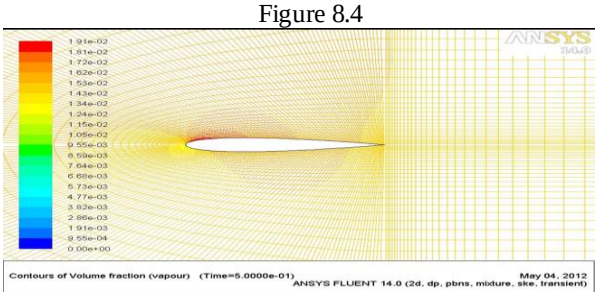

Figure 5

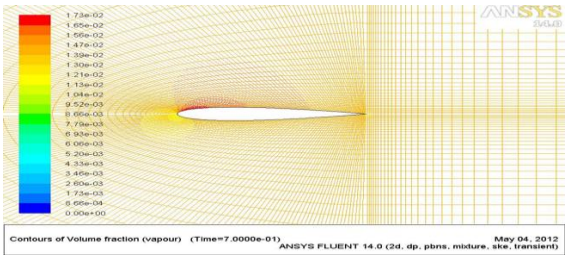

Figure 6

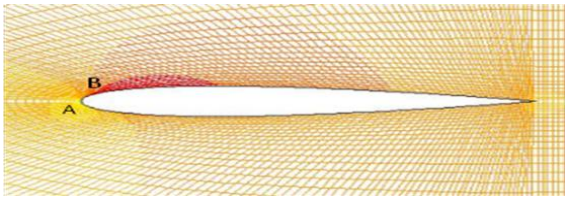

Figure 7

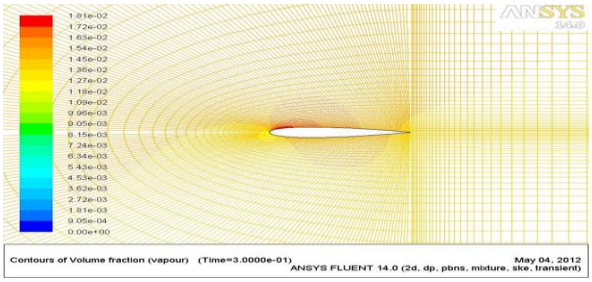

Figure 8

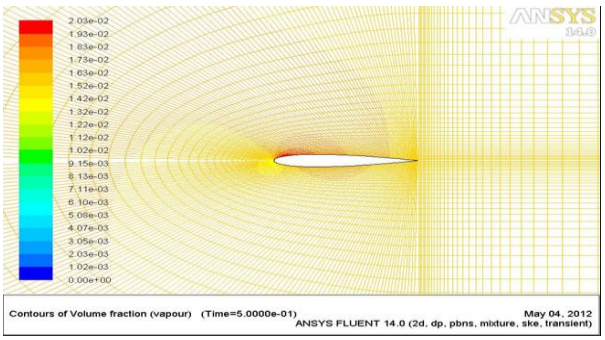

Figure 9

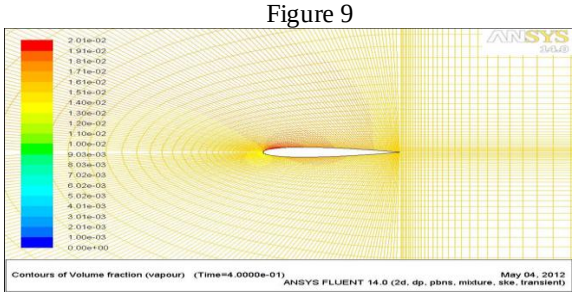

Figure 10

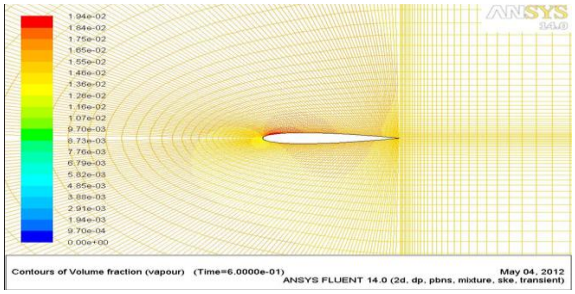

Figure 11

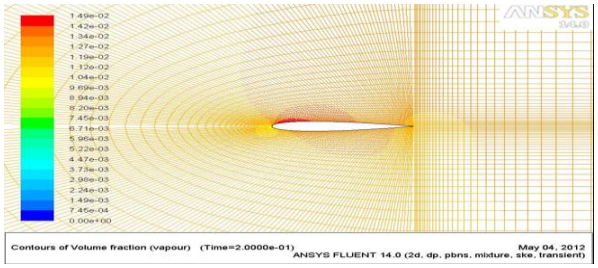

Figure 12

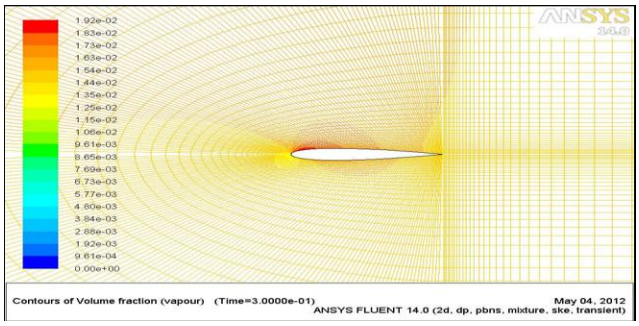

Figure 13

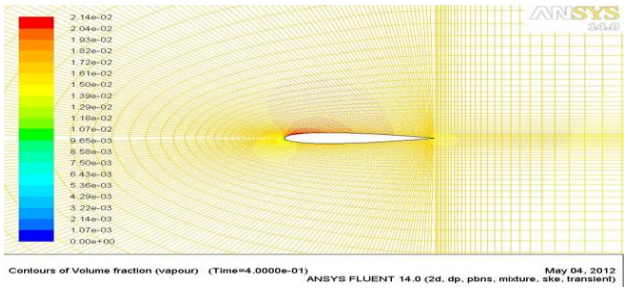

Figure 14

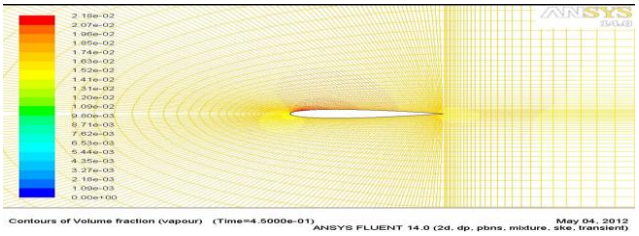

Figure 15

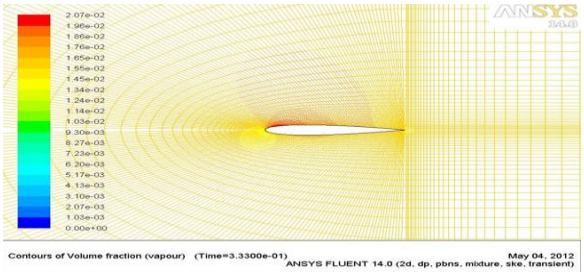

Figure15

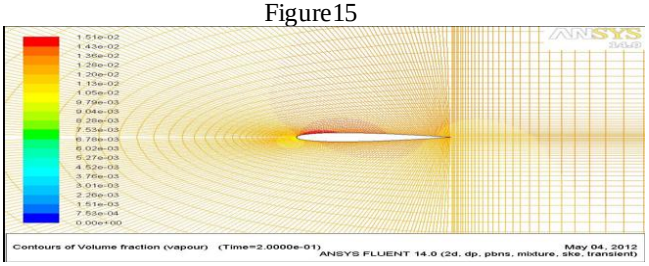

Figure 16

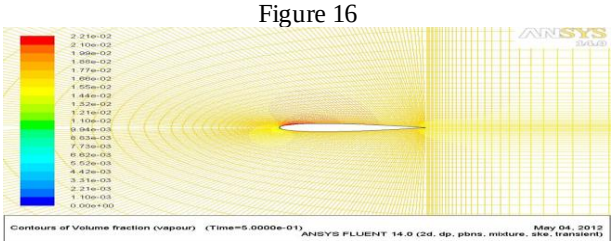

Figure 17

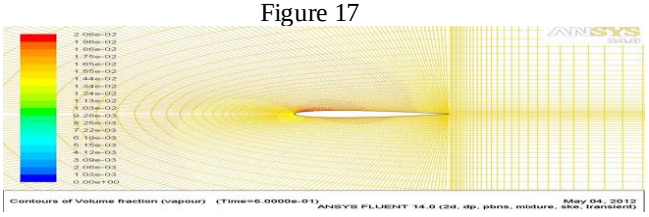

Figure 18

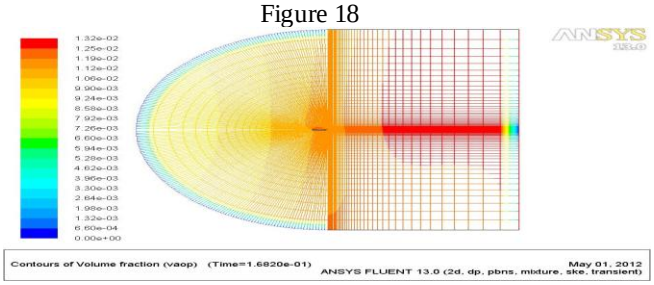

Figure 19

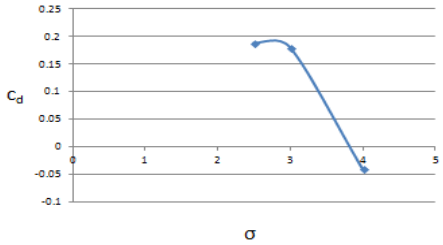

Figure 20(a)

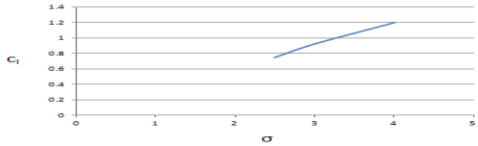

Figure 20(b)

Absolute pressure v/s position for different cavitation numbers

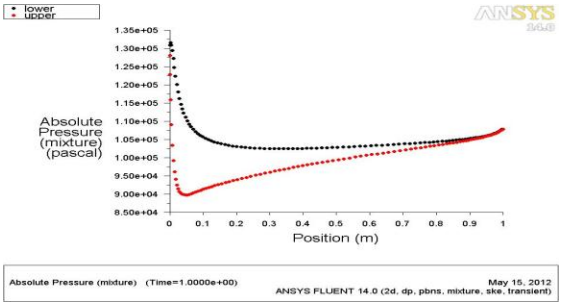

Figure 21(a)

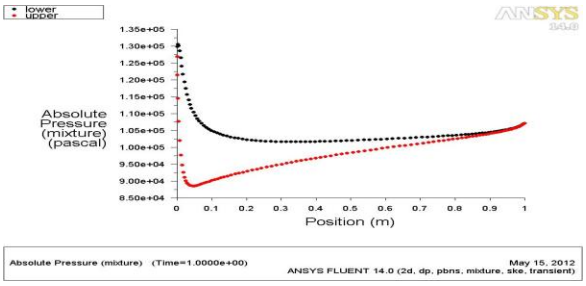

Figure 21(b)

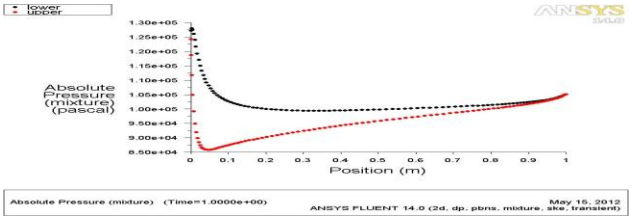

Figure 21(c)

Gas content-5ppm

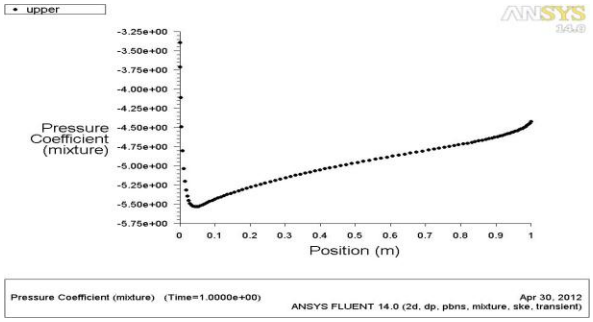

Figure 23(a)

Gas content-10ppm

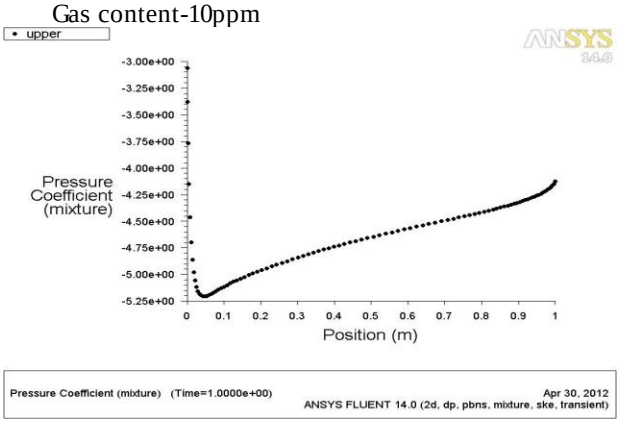

Figure 23(b)

Gas content-15ppm

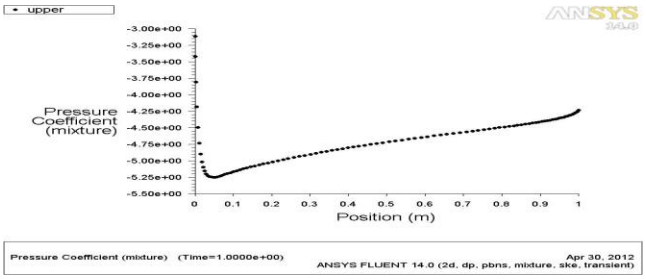

Figure 23(c)

Gas content-20ppm

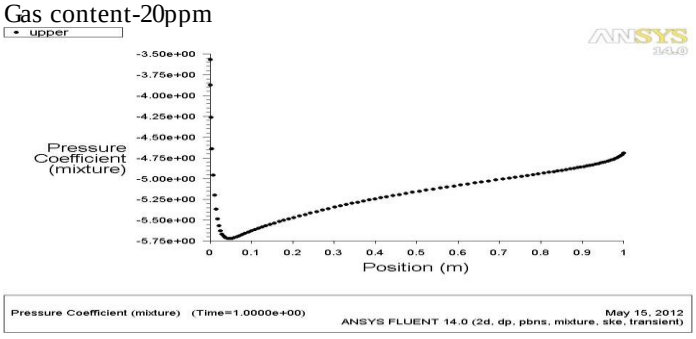

Figure 23(d)